

# Rotor-Stator-Interaction of a Radial Centrifugal Pump Stage with Minimum Stage Diameter

H. Roclawski  
 University of Kaiserslautern  
 Department of Mechanical Engineering  
 Gottlieb-Daimler-Strasse  
 67663 Kaiserslautern  
 GERMANY  
 roclaw@rhrk.uni-kl.de

D.-H. Hellmann  
 University of Kaiserslautern  
 Department of Mechanical Engineering  
 Gottlieb-Daimler-Strasse  
 67663 Kaiserslautern  
 GERMANY  
 hellmann@mv.uni-kl.de

**Abstract:** For radial multistage pumps with stationary vaned diffusers the diameter of the pump casing is much larger than the diameter of the impeller. In the case of submersible pumps, where just a limited space for installing the pump is available, smaller stator diameters need to be realized resulting in a loss in efficiency. Improving the design of these pumps and in order to save space and to decrease costs, alternative stators are being developed at the Institute of Turbomachinery and Fluid mechanics at University of Kaiserslautern. With respect to space, the optimum is a pump stage with a stage diameter equal to the outer impeller diameter. For realizing this concept, it is necessary for the flow to exit the radial impeller in axial direction before entering the stator. The advantage of this design is that when keeping the stage diameter constant, a much larger impeller diameter and thus a much higher hydraulic head can be realized. On the other hand, when keeping the hydraulic head or the specific speed constant, the diameter of the pump casing can be much smaller. In previous work, it was possible to increase the pump efficiency of these pump stages to values being comparable to conventional stators. In this paper the comparison to a conventional pump stage and the numerical analysis of the rotor-stator interaction of a pump stage with a small stage diameter is presented.

**Key-Words:** centrifugal pump, CFD, multistage pump, rotor-stator interaction

## 1 Introduction

Centrifugal pumps are build with several stages if the specific speed  $n_q$  (Eq. 1) for a specified capacity, head and speed drops under a certain limit. In this case the losses due to disk friction and gap flow in the spaces between impeller and casing are too high. Using several stages, the specific speed per stage is then located in a range with better efficiencies.

$$n_q = n * \frac{\sqrt{Q}}{\left(\frac{H}{i}\right)^{0.75}} \quad (1)$$

with  $Q$  in  $\left[\frac{m^3}{s}\right]$ ,  $H$  in  $[m]$ ,  $n$  in  $[min^{-1}]$  and number of stages  $i$   $[-]$ .

In order to direct the fluid to the next stage after exiting the impeller, stationary diffusers or volute casings are used. Due to the stator vanes the inner diameter of the casing  $D_{St}$  becomes much larger than the impeller diameter  $D_2$ . According to Gülich [1] the ratio of  $D_{St}/D_2$  can be calculated from Eq. 2

$$\frac{D_{St}}{D_2} = (1.05 \div 1.15) + 0.01 * n_q \quad (2)$$

In this paper a pump with a specific speed of  $n_q = 28 \text{ min}^{-1}$  is investigated. Therefore the ratio  $D_{St}/D_2$

should be between 1.33 and 1.43 when using a conventional stator. Looking at pumps which are currently build, also even larger ratios of  $D_{St}/D_2$  are used. In the special case of submersible pumps, where just a limited space for installing the pump is available, pumps are build with small ratios of  $D_{St}/D_2$  taking into account a loss in efficiency. With respect to space, the optimum is a stator with a diameter equal to the impeller diameter ( $D_{St}/D_2 \approx 1$ ). In the past, pumps of this kind have been designed and investigated the Institute of Turbomachinery and Fluid mechanics at University of Kaiserslautern. Fig.1 shows the meridional view of a conventional multistage centrifugal pump with  $D_{St}/D_2 = 1.5$  and a specific speed of  $n_q = 28 \text{ min}^{-1}$  compared to a pump stage with  $D_{St}/D_2 \approx 1$ . After exiting the impeller of a conventional pump stage the flow is decelerated in a radial diffuser for converting kinetic energy into static pressure. Then a crossover section and return channels are used for guiding the flow to the next pump stage. In case of the radial pump stage with  $D_{St}/D_2 \approx 1$  the casing diameter is reduced by 25% for obtaining the same specific speed. A gap of 0.5 mm between impeller and casing is present. The hub diameter at the impeller exit is reduced according to the impeller width, so that the fluid can exit the impeller in axial direction. Now the cross-over

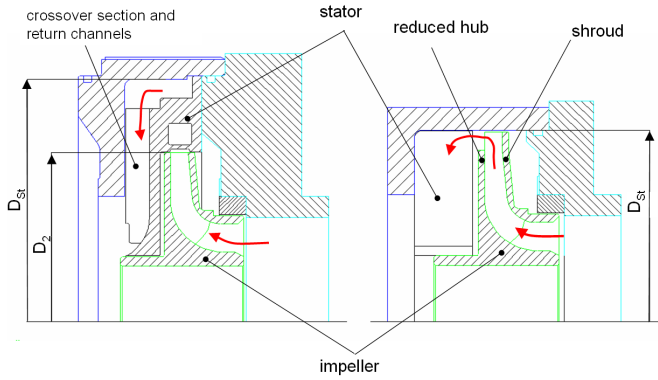


Figure 1: Comparison of a pump stage with conventional stator to a pump stage with  $D_{St}/D_2 \approx 1$

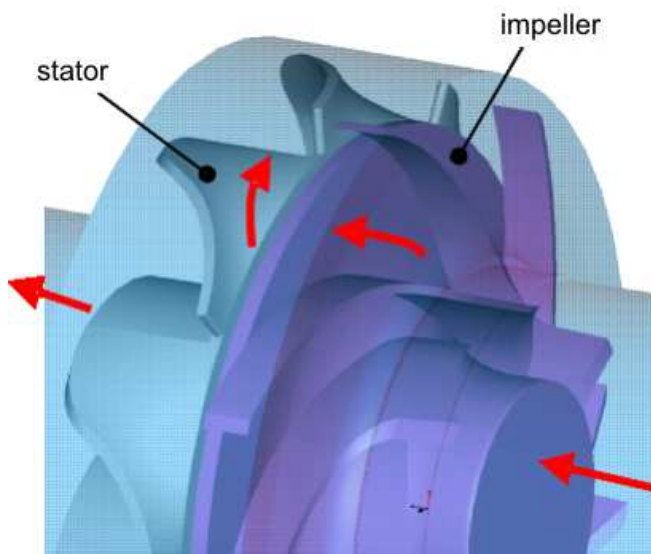


Figure 2: 3-dimensional model of the pump stage

section becomes part of the impeller. The distance between impeller and stator is 4 mm. Fig.2 shows a 3-dimensional CAD-model of the pump stage. The impeller shroud is not shown. For simplicity, two-dimensional blades are used for the seven vanes of the impeller. The stator is built with nine vanes. Both, impeller and stator are designed according to practical values obtained in experimental investigations at University of Kaiserslautern. Due to the high angular momentum of the flow at the impeller exit, the leading edge of the stator vanes are oriented in radial direction first. After the fluid enters the stator, the blades are turned into axial direction for guiding the flow towards the shaft.

The advantage of this design is that for the same specific speed, larger impellers can be build while the casing diameter is reduced. So far, there is only little knowledge of the flow in these pump stages. There-

fore in this paper, the rotor-stator interaction based on CFD results is presented.

## 1.1 Previous work

The design of centrifugal pumps is usually based on empirical data obtained from the long lasting experience of pump manufacturers. Currently there is no data in the literature available for designing the kind of pump investigated here. Therefore, for improving the efficiency of these pumps, the first task is to gain reliable data for developing a design method for the new stators. This can be done by experiment and simulation. Compared to experiments, with CFD it is possible to calculate many variations of the stator in a shorter time and at lower costs. However, due to the uncertainties in numerical modeling, the CFD model needs to be validated with experimental data. Once a reliable CFD model has been obtained, several variations of the stator can be calculated.

For the validation, two test rigs are available at University of Kaiserslautern. Different concepts of stator vanes can be investigated by means of hot-wire anemometry and measurements of characteristic curves. For reducing costs, the test rigs are operated with air instead of water in compliance with the similarity laws.

Using CFD, it was found that a large flow separation occurs in all stator channels causing the pump efficiency to be 20% lower in the point of best efficiency compared to conventional multistage centrifugal pumps with  $D_{St}/D_2 = 1.5$  during operation with air. After adjusting the design method according to the numerical results, a new stator was designed by [2]. With this stator the pump efficiency is comparable to these of a pump stage with conventional stator ( $D_{St}/D_2 = 1.5$ ). This was shown by CFD and experiment in [3].

Fig.3 shows the hydraulic head of the optimized pump stage compared to the initial design and the conventional stator. The measurements of the pump stage with conventional stator were carried out by [4]. The characteristic curve was calculated by means of CFD first. The CFD results show that the hydraulic head is increased by about 35% compared the conventional pump stage. After obtaining these promising results, the stator was investigated experimentally. The measurements show an increase by 28%. Comparing the pump efficiencies (Fig.4), with the optimized stator a large improvement in pump efficiency is achieved. With a value of 98% of the efficiency of the conventional stator, the pump stage with the small stator is now located in a range of conventional radial pump stages. The point of best efficiency is located at  $1.3 \cdot Q_{opt}$  of the conventional pump stage. The specific speed is  $n_q = 30 \text{ min}^{-1}$ .

One should be aware of that these results were obtained with an impeller with just 2D-cylindrical

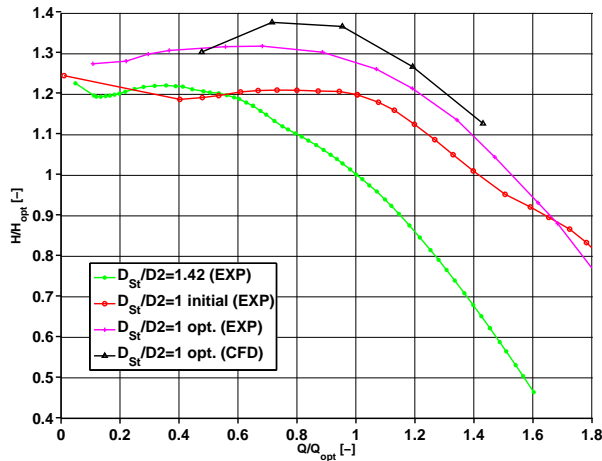


Figure 3: Q-H-characteristic curve

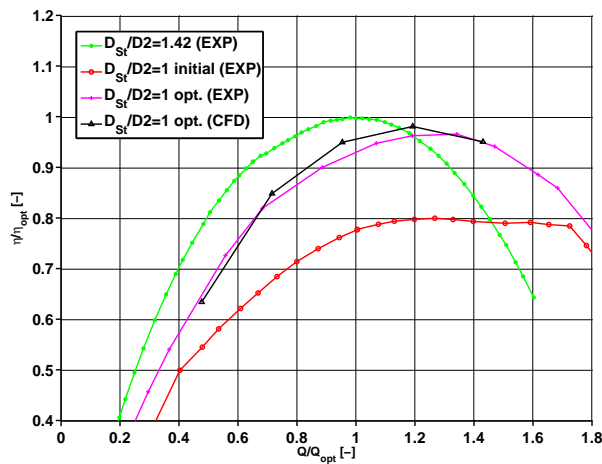


Figure 4: Hydraulic Efficiency

blades, whereas for the conventional pump stage an impeller with 3-dimensional shaped blades was used. After improving the stator design, for future investigations an impeller with 3-dimensional shaped blades will be investigated.

## 2 Numerical Model

All calculations have been carried out using the commercial CFD-code Fluent 6.2. Starting from a converged frozen rotor solution, the sliding-mesh model was used for analyzing rotor-stator interaction. Due to the fact that the number of impeller and stator blades has no common factor, the usage of periodic boundary conditions is not appropriate. Furthermore, Dupont[5] showed that in this case the unsteadiness is not exactly the same in the neighboring blade passages. Therefore, the whole geometry is modeled. The impeller is meshed with hexahedral cells includ-

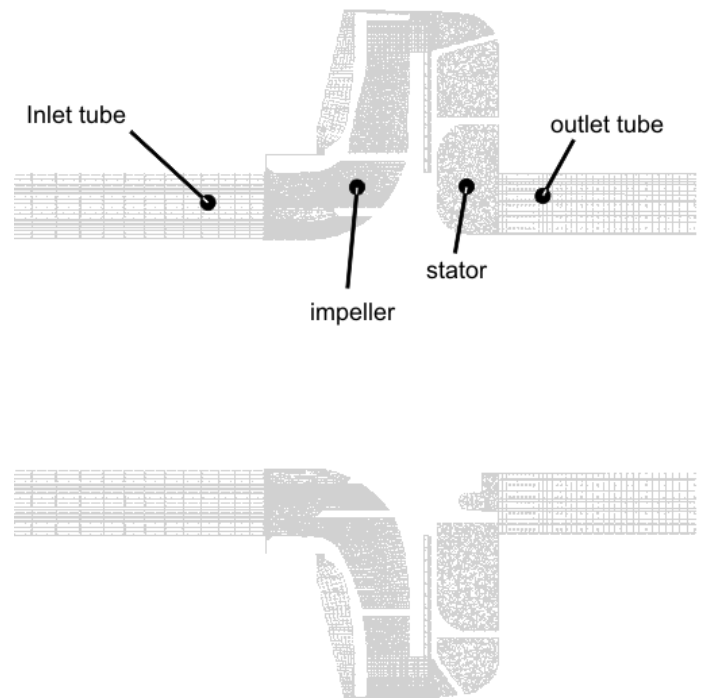


Figure 5: CFD-model including pump cavities

ing the spaces between impeller and casing on pressure and suction side. In case of the stator, the axial gap between stator and shaft was neglected. For the optimization of the pump stage, it was necessary to calculate many variations of the stator. Since modern CFD-codes can handle unstructured meshes, tetrahedral cells are used for keeping the meshing effort of the stator variations low. Fig.5 shows the mesh of the pump stage. Grid interfaces are used to connect the rotating domain of the impeller to the inlet tube, the impeller side gaps and the stator.

At the inlet and outlet boundaries, the computational domain is extended to  $6 \cdot D$  to obtain a fully developed velocity profile. The flow is assumed to be incompressible. Therefore it is possible to use the outflow boundary condition of Fluent at the outlet of the computational domain. At the inlet, the velocity is specified. The impeller speed is  $3500 \text{ min}^{-1}$ . All calculations are performed with the segregated solver of Fluent using a 2nd order discretization scheme and the Standard  $k-\epsilon$ -model.

A numerical solution of the governing equations is always an approximation because not the integral equations are solved, but their discretized form. Therefore the quality of this approximation needs to be examined. In CFD one can distinguish between the modeling, discretization and solver error.

The discretization error is analyzed by comparing results on 6 different meshes using a 1st order and a 2nd order discretization scheme. It is found that for a grid with 2,900,000 cells the solution is grid inde-

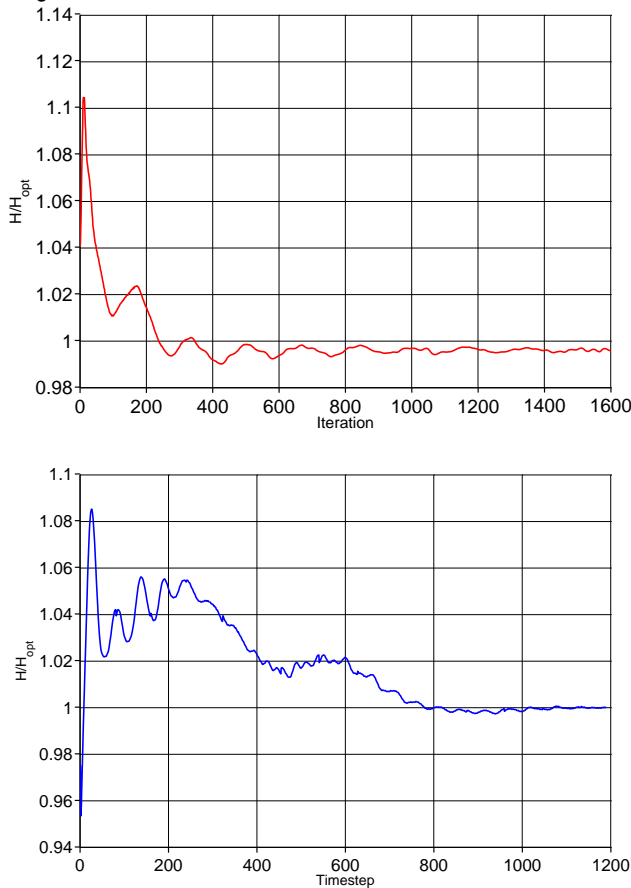


Figure 6: Using hydraulic head for judgment of convergence

pendent. In this case  $y^+$  is in a range between 10 and 250. In order to minimize the solver error, all calculations are performed with a double precision solver. The residuals and the hydraulic head as well as efficiency are monitored to judge convergence. Fig.6 shows the influence of the specified convergence criterion or rather the influence of the number of iteration steps on the hydraulic head for frozen rotor and sliding mesh calculations. In the frozen rotor case, one can see the asymptotic convergence to a limiting value. For calculations using the sliding mesh model a time periodic solution has to be achieved. The time step size was set to one degree of impeller rotation. For each time step it took about 25 iterations until the convergence criterion of  $10^{-4}$  is met. For achieving a time periodic solution, 2.5 impeller rotations are necessary.

The modeling error occurs due to the usage of models for processes which are not resolved by the mesh (e.g. turbulence, geometrical details, etc.). Modeling errors can be influenced by the user, but they are difficult to estimate numerically. Therefore it takes experimental data for the validation of the numerical model. In the case of the pump stage, the model was validated by means of hot-wire anemom-

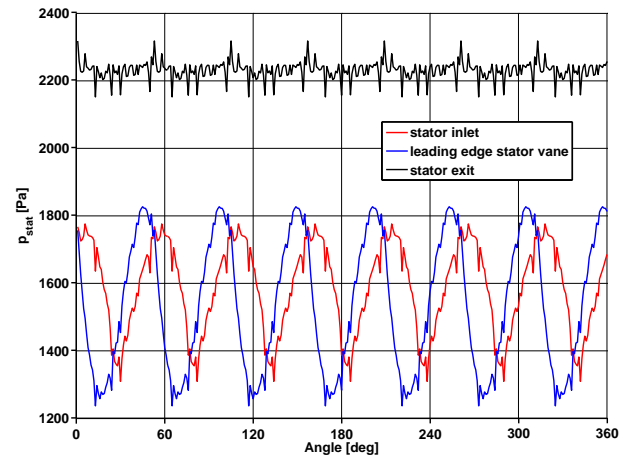


Figure 7: Pressure fluctuations at monitor points

etry and measurements of characteristic curves. The validation of the CFD-model was presented in detail in [6].

### 3 Rotor-Stator-Interaction

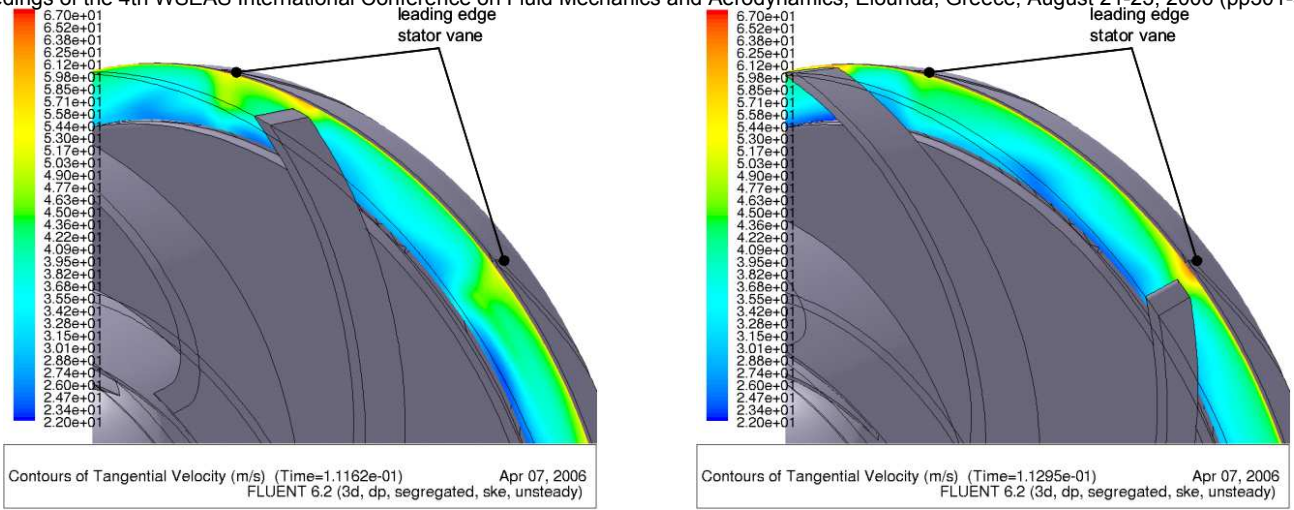
For investigating the pressure fluctuations in the pump stage, three monitor points were defined. The points are located at half blade height between two vanes at the stator inlet, at the leading edge of a stator vane and at the stator exit. Fig. 7 shows the monitored static pressure during one impeller rotation. As expected, higher values of static pressure are present at the stator exit. At the two inlet monitors, both signals have the same frequency, but at the leading edges of the stator vanes the amplitude is slightly higher. The shift in phase occurs according to the different monitor position in circumferential direction. In general, the fluctuations at these two monitor points are more explicit than at the stator exit.

The frequency spectra obtained by FFT analysis for all three monitor points are shown in Fig.8. Clearly, the impeller frequency  $f_{im}$  which can be calculated from Eq. 3 and its multiples can be identified. This is also true for centrifugal pumps with conventional stator and pumps with volute casings as shown in [7] and [8].

$$f_{im} = \frac{n}{60} * z_{im} = 408, \bar{3} Hz \quad (3)$$

with frequency  $f_{im}$  in  $[Hz]$ , speed  $n$  in  $[min^{-1}]$  and number of blades  $z_{im}$  [-]. The highest amplitudes are present at the leading edge of the stator vane. The amplitude at the stator exit is negligible small.

For a further investigation of the interaction between rotor and stator, the circumferential ( $c_u$ ), axial ( $c_{ax}$ ) and radial ( $c_r$ ) velocity components are ana-



(a)  $C_u$  at position 1

(b)  $C_u$  at position 1 + 28°

Figure 9: Circumferential velocity contours

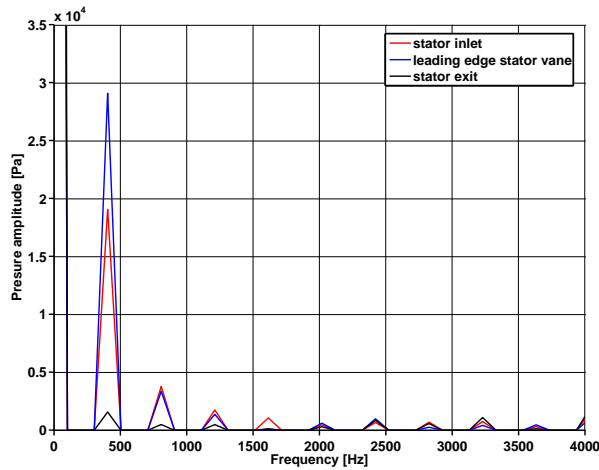


Figure 8: Frequency spectra of static pressure at monitor points

lyzed in a plane between impeller and stator. Fig.9 shows a contour plot of the circumferential velocity component at two different impeller positions. It can be seen that the circumferential velocity increases with increasing impeller diameter. The maxima are located at the outer diameter of the leading edge of the stator vanes and at the trailing edge of the impeller vanes. Their values of the impeller speed  $u_2$  squared are present. Considering the interaction of impeller and stator, it can be seen from Fig.9(b) that during the impeller rotation  $c_u$  becomes maximal every time an impeller vane passes the leading edge of a stator vane.

Contour plots of axial velocity between impeller and stator for different impeller positions are shown in Fig.10. Blue regions indicate negative axial velocities. As for the circumferential velocity, axial velocity increases with increasing impeller diameter. The highest axial velocities are present at the outer diameter at the pressure side of the impeller vanes. In addition, nine regions of reversed flow are present at the inner diameter of each leading edge of the stator vanes. Furthermore, more regions of reversed flow can be observed at the suction side of the impeller vanes. This is also true when just calculating the impeller without stator as shown in [6]. The reason for the reversed flow is the low pressure region at the suction side of the impeller vanes. The flow back into the impeller depends on the position of the rotor relative to the stator. Figs. 10(a) to 10(d) show that the reversed flow is enhanced when an impeller vane passes a stator vane. Then also the high axial velocities at the pressure side of the impeller vanes are reduced, due to the blockage of the stator. After passing the stator vane, the axial velocity increases at the pressure side of the impeller vane. On the suction side of the impeller vane, axial velocity decreases at the entrance of a stator channel during impeller

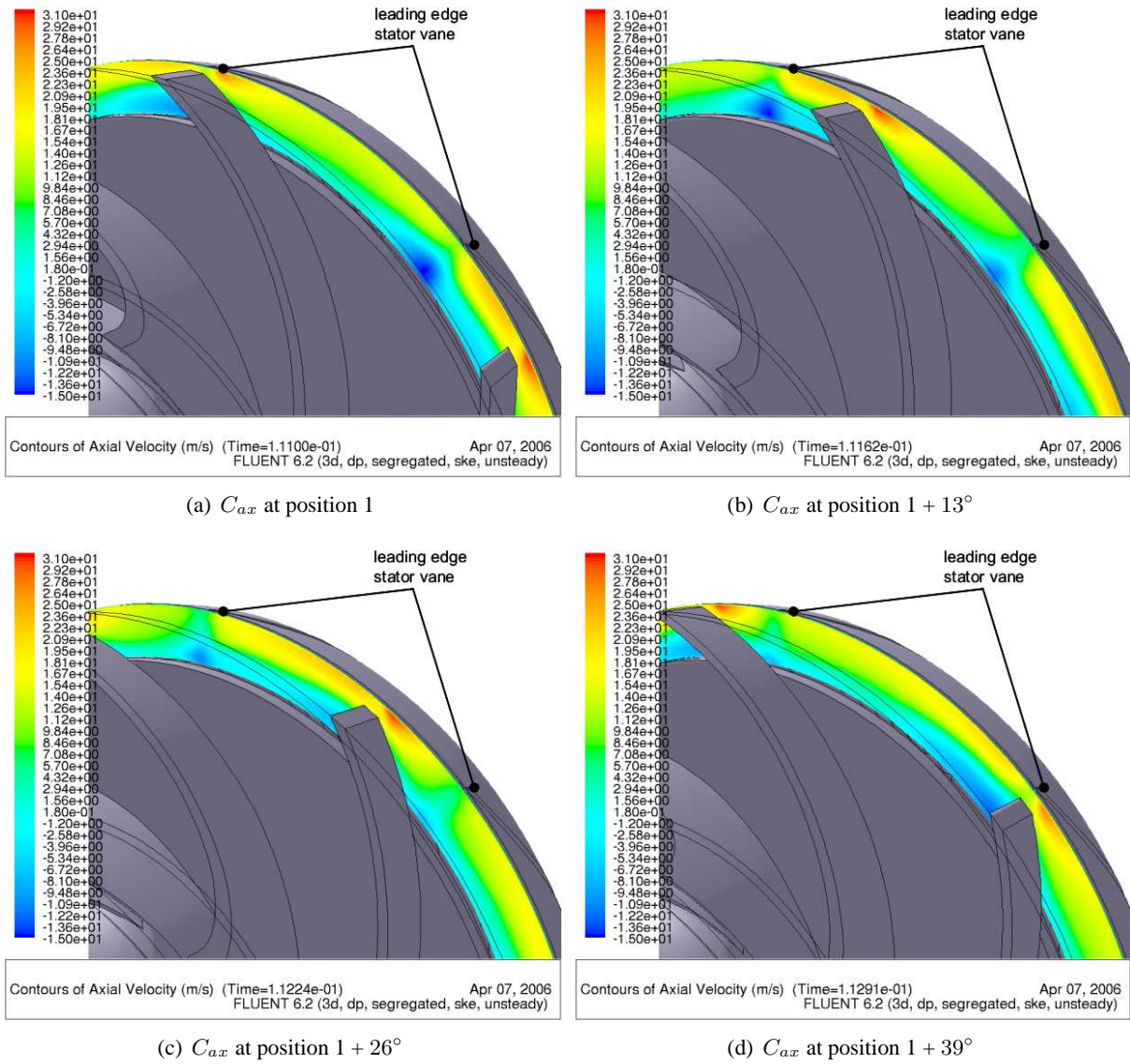


Figure 10: Axial velocity contours

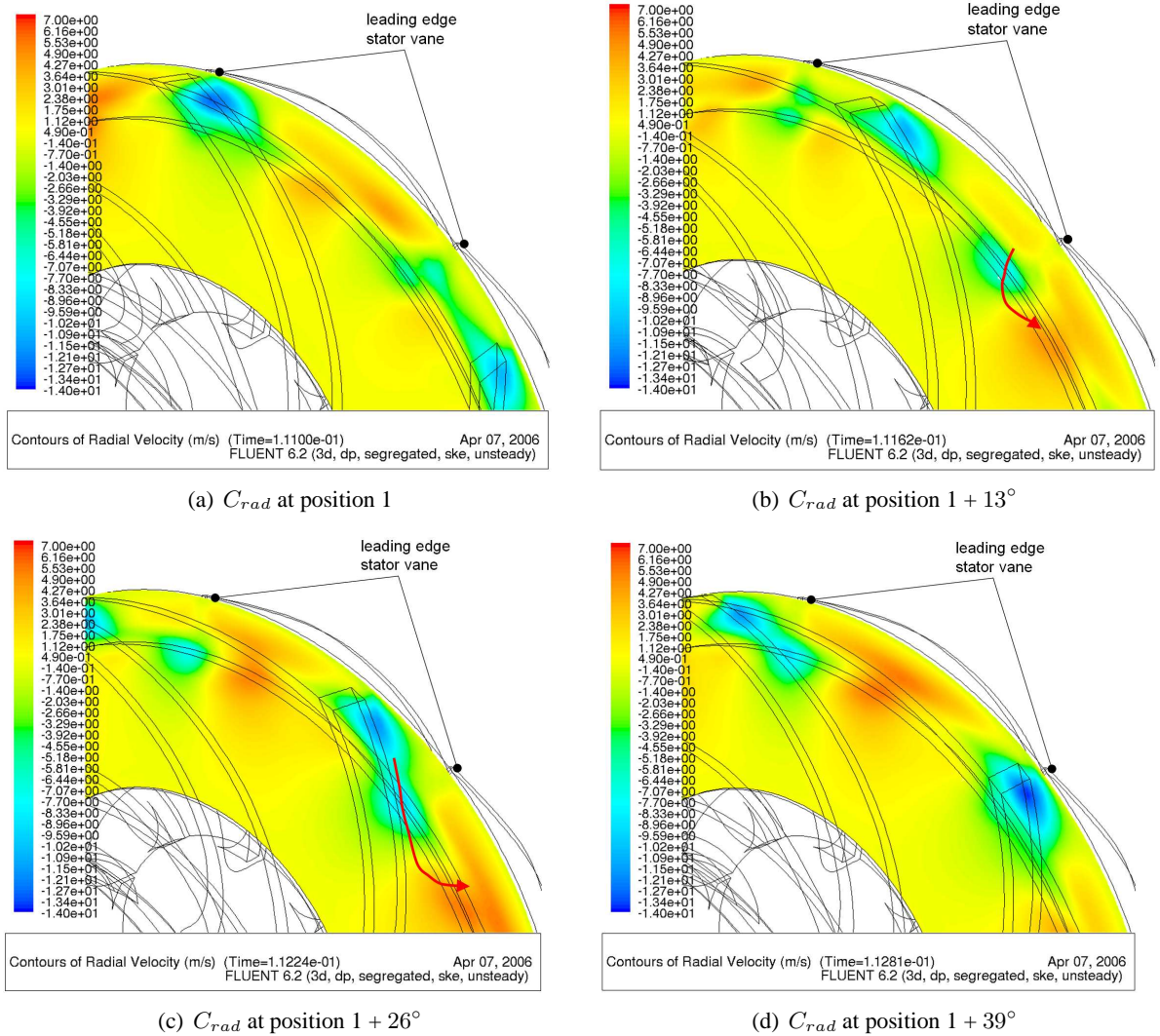


Figure 11: Radial velocity contours

rotation until it is increased by the next impeller vane again.

Fig.11 shows contour plots of radial velocity. In this case the impeller and stator is shown as wire frame model in order to visualize radial velocity in the gap between impeller and stator. Negative signs indicate a flow towards the shaft, positive signs represent flow outwards. In general, flow towards the shaft can be observed at the leading edges of the stator vanes and at the suction side of the impeller vanes as shown in Fig.11(a). While an impeller vane approaches the leading edge of a stator vanes, the region and the magnitude of flow towards the shaft at the stator vanes is increased (Figs.11(b) and 11(c)). When the impeller vane is close enough, these two regions unite as shown in Fig.11(d). Due to the blockage of the stator vane, the flow is displaced into the gap between stator and rotor. Behind the leading edges of the stator vanes the flow is driven outwards again (red regions in Figs.11(a) to 11(d)).

Summarizing the observations made for all three velocity components, one can state that circumferential velocity increases with increasing impeller diameter. Thus, at larger diameters the flow contains more energy. Due to the pressure difference between pressure and suction side an energy balance occurs. When exiting the impeller, a part of the high energy containing fluid from the pressure side displaces the flow in the low pressure region of the suction side into the gap between impeller and stator (negative  $c_{rad}$ ) and leads to a reversed flow into the impeller (negative  $c_{ax}$ ). This effect becomes stronger when an impeller blade passes the leading edge of a stator vane. Due to the blockage of the leading edge of the stator vanes, the flow which cannot enter the stator is too high and due to the small gap between impeller and stator, the flow displacement is enhanced.

## 4 Conclusion

The rotor-stator interaction of a centrifugal pump with minimum stage diameter has been investigated by analyzing CFD-data. The CFD calculations have been performed using the sliding mesh model of the commercial code Fluent 6.2. The results have been validated by measurements of characteristic curves and hot-wire data. It was shown that with this type of stator the casing diameter can be reduced by 25% while concurrently larger impeller diameters can be build leading to a higher hydraulic head. Furthermore, the efficiency of the pump stage is comparable to conventional stators with much larger stage diameters.

Analyzing the pressure fluctuations at three monitor points in the stator, it was shown by FFT-analysis that the fluctuations are dominated by the impeller fre-

quency. By analyzing the velocity components in a plane between impeller and stator it was shown that circumferential velocity increases with impeller diameter. Values of  $u_2$  squared are present at the leading edges of the stator vanes. Investigating axial and radial velocities, the existence of a balancing flow between high energy containing fluid from the pressure side to the low pressure region on the suction side of the impeller vanes leading to negative axial and radial velocities was described. This exchange flow is enhanced when an impeller blade passes the leading edge of a stator vane. In the future, it is planed to compare the numerical results to hot-wire data and to investigate rotor-stator interaction at partload and overload conditions. Besides the analysis of rotor-stator interaction, different impeller designs will be investigated for obtaining a deep understanding of the flow physics in the pump stage.

### References:

- [1] Gülich, J., 1999. *Kreiselpumpen*. Springer Verlag.
- [2] Weiten, A., 2005. Unpublished results. TU Kaiserslautern.
- [3] Roclawski, H., Weiten, A., and Hellmann, D.-H., 2006. "Numerical Investigation and Optimization of a Stator for a Radial Submersible Pump Stage with Minimum Stage Diameter". In Proceedings of ASME FEDSM06.
- [4] Weinert, K., 2002. Unpublished results. TU Kaiserslautern.
- [5] Dupont, P., 2005. "Rotor-Stator Interaction in a vaned diffuser radial flow pump". In Proceedings of ASME FEDSM2005.
- [6] Roclawski, H., and Hellmann, D.-H., 2006. "Numerical Simulation of a Radial Multistage Centrifugal Pump". In 44th AIAA Aerospace Sciences Meeting and Exhibit, AIAA 2006-1428.
- [7] Benra, F.-K., and Dohmen, H., 2005. "Numerical Investigation of the Transient Flow in a Centrifugal Pump Stage". In Proceedings of ASME FEDSM2005.
- [8] Aysheshim, W., and Stoffel, B., 2000. "Numerical and Experimental Investigation on a Centrifugal Pump Stage with and without a Vaned Diffuser: Experimental Part ". In Proceedings of 20th IAHR-Symposium, paper No. CFDD-G01.